

## Accurate Simulation of Thermal Neutron Filter Effects In the Design of Research Reactor Beam Applications

A. I. Hawari\*, I. I. Al-Qasir and K. K. Mishra

North Carolina State University, Department of Nuclear Engineering, Raleigh, NC 27695, USA

### Abstract

Thermal neutron filters are routinely used for spectral shaping in neutron beam applications. In many situations, the neutron source is the core of a research reactor that faces several beamports. Consequently, the neutrons leaking into the beamport will have an energy spectrum that extends over several decades from the low energy (thermal) range to the high energy (fast) range that is typical of prompt fission neutrons. At the PULSTAR reactor of North Carolina State University, sapphire and bismuth filters are used within the beamports to reduce the epi-thermal and fast neutron components and gamma-rays. The main objective is to produce thermal neutron beams with a high neutron-to-gamma ratio. The thermal beams are used to drive facilities for neutron imaging and neutron diffraction. To assure that these facilities are accurately designed, thermal neutron scattering cross section libraries are generated for sapphire and bismuth at 300 K. The libraries do not account for coherent elastic (i.e., "Bragg") scattering, which is equivalent to assuming the use of a single crystal filter with a preferential orientation relative to the neutron beam. MCNP Monte Carlo simulations show that, using the created libraries, the phenomenon of neutron filtration can be captured and diagnosed to ensure accurate beam and facility designs.

**KEYWORDS:** *Research reactor, neutron beam, thermal neutron, neutron filter, scattering law, sapphire, bismuth*

### 1. Introduction

Research reactors are utilized as neutron sources for various applications. Usually, the neutrons are guided using beamports to form beams that can be used in experimental stations that are located at the end of the port. In general, the neutrons in a given beam will have an energy spectrum that extends over several decades from the low energy (thermal) range to the high energy (fast) range that is typical of prompt fission neutrons. However, many of the applications that are implemented in research reactors require that the neutron beam is filtered to facilitate the transmission of spectral components that are of interest to the application and remove other components from the spectrum. Examples of such applications include thermal neutron radiography, prompt gamma neutron activation analysis, and neutron diffraction to name a few.

The design and setup of facilities to implement such applications is guided by computational

---

\* Corresponding author, Tel. 919-515-4598, Fax. 919-513-1276, E-mail: [ayman.hawari@ncsu.edu](mailto:ayman.hawari@ncsu.edu)

simulations that aid in optimizing the design and predicting the performance characteristics of a particular facility. Nevertheless, if a neutron beam filter is used in the design, then the accuracy of such simulations will depend on accurate modeling of the interaction of the neutrons with the filter. The accurate simulation of the interaction processes (absorption, scattering, etc.) necessitates the use of the appropriate neutron cross section libraries for a given filter material. Specifically, for thermal neutron filters, accurate description of the scattering of thermal neutrons will be essential to ensure the fidelity of the simulation.

In general, a neutron filter will preferentially pass neutrons with energies that correspond to a minimum in the total cross section while greatly attenuating neutrons with energies that deviate from that minimum. For thermal neutrons, a material that has a small absorption cross section and can be formed into large and near perfect single crystals represents the filter of choice. In this case, coherent elastic scattering of the neutrons (i.e., “Bragg” scattering) can be minimized by preferentially orienting the crystal relative to the neutron beam, while if necessary inelastic scattering can be reduced by cooling the crystal to limit the availability of phonons. Consequently, a practical cross section library that describes thermal neutron interactions in such a material would include information on the absorption and inelastic scattering of the neutrons. The absorption cross sections are usually given by the elemental cross section libraries that are supplied with the computer codes (e.g., the libraries supplied with the MCNP Monte Carlo code). However, for many materials that are important to nuclear technology, the inelastic thermal neutron scattering cross sections are not readily available. A modern computational approach for estimating these cross sections has been previously presented [1].

## 2. Inelastic Thermal Neutron Scattering Cross Sections

Filter materials such as sapphire and bismuth have found extensive utilizations in the creation of thermal neutron beams. In addition, bismuth is frequently used as a gamma-ray filter. To enable the computational simulation of the neutron filtering effect of these materials, thermal neutron scattering cross-section libraries must be created in the appropriate formats that can be accessed by typical neutronics computer codes. Assuming conditions that result in minimizing Bragg scattering, the inelastic scattering component becomes the dominant factor in these libraries.

### 2.1 Sapphire

Large sapphire single crystals are used as thermal neutron filters. In addition, it was experimentally demonstrated that for a sapphire crystal with the [001] axis oriented parallel to the neutron beam, Bragg scattering is minimal [2]. Furthermore, it has been established that cooling the crystal does not result in substantial gains in its transmission efficiency for thermal neutrons [3]. Therefore, sapphire represents an efficient and convenient filter to implement. Sapphire ( $\alpha$ -Al<sub>2</sub>O<sub>3</sub>) has a rhombohedral unit cell that belongs to the trigonal system with space group  $R\bar{3}c$ . Its unit cell contains two molecules (Al<sub>2</sub>O<sub>6</sub>), where each aluminum ion is surrounded by 6 oxygen ions, and each oxygen ion is surrounded by 4 aluminum ions. The structure can also be viewed as a stacking of aluminum and oxygen atoms in a hexagonal unit cell with three times the size of the rhombohedral unit cell. The lattice parameters of the  $\alpha$ -Al<sub>2</sub>O<sub>3</sub> rhombohedral unit cell are  $a=b=c= 5.127 \text{ \AA}$ , and  $\alpha=\beta=\gamma= 55.25^\circ$ . This corresponds to

$a=b= 4.754 \text{ \AA}$ ,  $c= 12.99 \text{ \AA}$ ,  $\alpha=\beta= 90^\circ$ , and  $\gamma= 120^\circ$  for the hexagonal cell [4]. Figure 1 shows the  $\alpha\text{-Al}_2\text{O}_3$  rhombohedral unit cell and the corresponding hexagonal cell.

The calculations of the inelastic scattering cross sections for sapphire were performed using the NJOY code system [5,6]. The calculation is based on phonon frequency distributions derived from simulations that were carried out using the ab initio density functional theory code VASP and the lattice dynamics code PHONON [7,8]. The ab initio calculation was performed using the generalized gradient approximation (GGA), and projector augmented wave (PAW) pseudopotential. The calculations are based on a  $2 \times 2 \times 2$  supercell with 80 atoms. A plane-wave basis set with a 500 eV energy cutoff was applied. Integration over the Brillouin zone was confined to the  $3 \times 3 \times 3$  k-mesh points generated by the Monkhrust Pack scheme [9]. The supercell symmetry and the site symmetry of the non-equivalent atoms reduced the number of displacements required to calculate Hellmann-Feynman (HF) forces. In the case of  $\alpha\text{-Al}_2\text{O}_3$  six independent displacements along the x, y, and z directions for aluminum and oxygen were used with displacement amplitudes of  $0.03 \text{ \AA}$ . Each displacement generated 240 force components; hence six displacements gave 1440 HF force components.

The generated HF forces are used by the PHONON code for calculating the force constants and constructing the dynamical matrix, by utilizing the crystal symmetry space group and assuming a finite range of interaction. The partial and total densities of states were obtained using 50,000 wave vectors, generated randomly in the first Brillouin zone. Figure 2 shows the partial phonon frequency distributions of aluminum, and oxygen in  $\alpha\text{-Al}_2\text{O}_3$ , and the total phonon frequency distribution of  $\alpha\text{-Al}_2\text{O}_3$ . As it can be seen, the phonon frequency distribution is characterized by three regions, the first one is below  $\sim 0.041 \text{ eV}$ , where the main contribution to this region comes from the aluminum atoms (larger mass). The second region is between  $0.041 \text{ eV}$  and  $0.088 \text{ eV}$ , which is the main region for both oxygen and aluminum atoms to vibrate. Nearly  $2/3$  of the vibrations are taking place in this region. The third region is above  $0.088 \text{ eV}$  and is characterized by a strong Van Hove singularity at  $0.093 \text{ eV}$ . Figure 3 shows the total neutron cross section per molecule of  $\alpha\text{-Al}_2\text{O}_3$  at 300 K. The calculation is compared to experimental data for various grades of sapphire and shows general good agreement.

**Figure 1.**  $\alpha\text{-Al}_2\text{O}_3$  (a) Rhombohedral and (b) Hexagonal unit cells. The Al atoms are yellow and the O atoms are red.

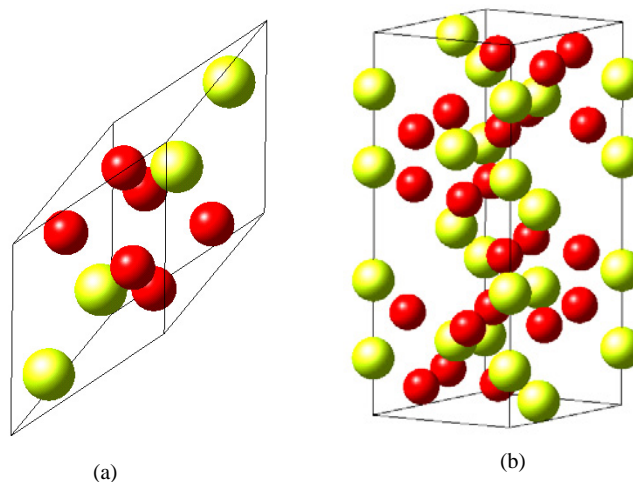


**Figure 2.** (a) The partial frequency distributions for Al and O in  $\alpha$ -Al<sub>2</sub>O<sub>3</sub>, and (b) the total phonon frequency distribution for  $\alpha$ -Al<sub>2</sub>O<sub>3</sub>.

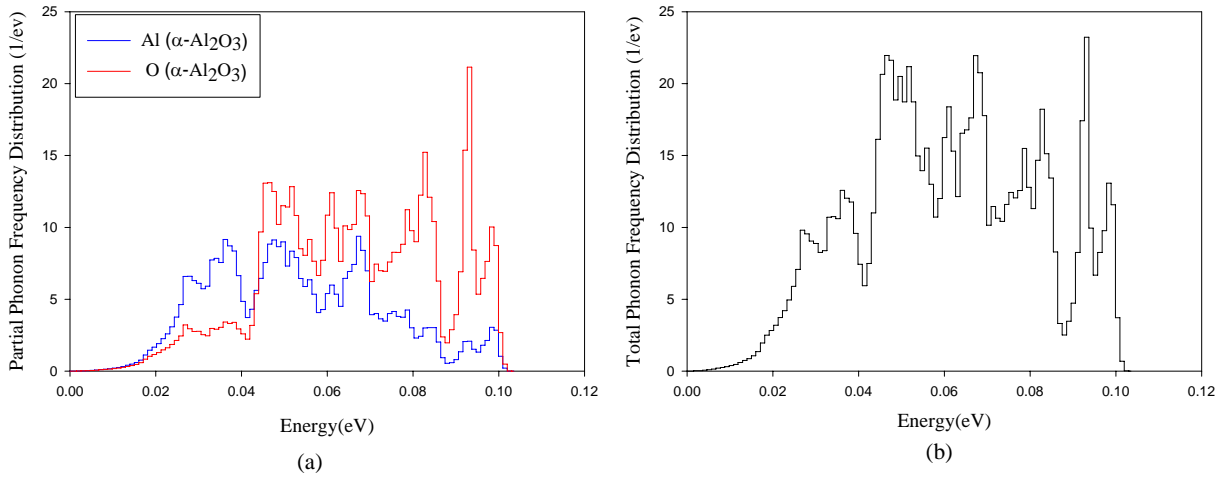
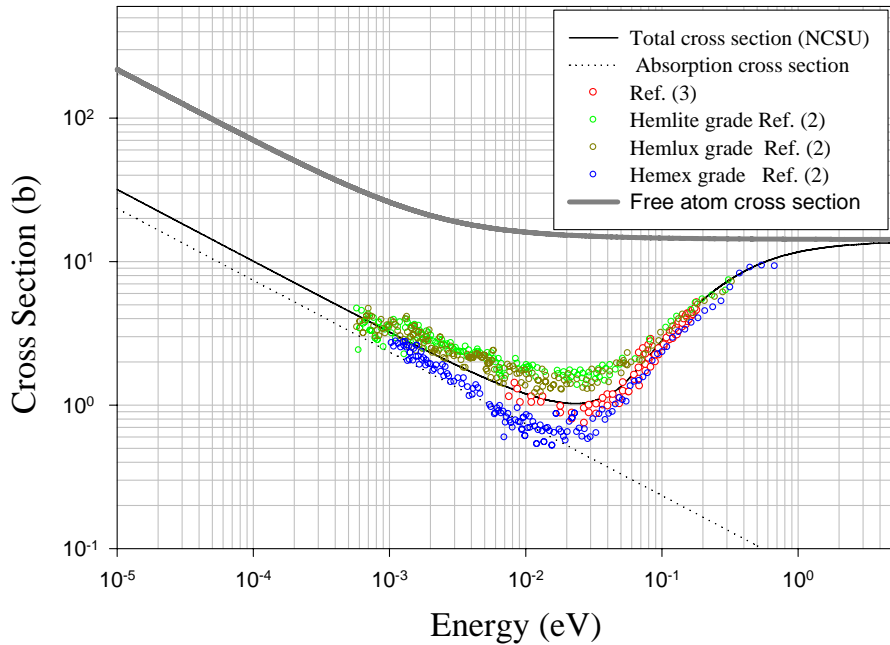


**Figure 3.** Total cross section per molecule for a sapphire single crystal ( $\alpha$ -Al<sub>2</sub>O<sub>3</sub>) at 300 K. Coherent Elastic (Bragg) scattering is assumed to be negligible.



## 2.2 Bismuth

Bi belongs to the semimetal  $V_B$  group. It has a rhombohedral unit cell that belongs to the trigonal system with space group  $R\bar{3}c$ . It has two atoms per unit cell. Similar to sapphire its lattice can be viewed as a hexagonal unit cell. The lattice parameters of the Bi rhombohedral

unit cell are  $a=b=c = 4.724 \text{ \AA}$ , and  $\alpha=\beta=\gamma = 57.35^\circ$ . This corresponds to  $a=b = 4.533 \text{ \AA}$ ,  $c = 11.797 \text{ \AA}$ ,  $\alpha=\beta = 90^\circ$ , and  $\gamma = 120^\circ$  for the hexagonal cell [4]. Figure 4 shows the Bi rhombohedral unit cell and the corresponding hexagonal one.

The calculations of the inelastic scattering cross sections for bismuth were performed using the NJOY code system [5,6]. The calculation is based on phonon frequency distributions derived from simulations that were carried out using the ab initio density functional theory code VASP and the lattice dynamics code PHONON [7,8]. The ab initio calculation was performed using the generalized gradient approximation (GGA), and projector augmented wave (PAW) pseudopotential. The calculations are based on a  $2 \times 2 \times 2$  supercell with 16 atoms. A plane-wave basis set with a 243 eV energy cutoff was applied. Integration over the Brillouin zone was confined to the  $4 \times 4 \times 4$  k-mesh points generated by the Monkhrust Pack scheme [9]. Three independent displacements along the x, y, and z directions were used with displacement amplitudes of  $0.03 \text{ \AA}$ . Each displacement generated 144 HF force components.

The phonon frequency distribution was obtained by using  $10^5$  wave vectors, generated randomly in the first Brillouin zone. Figure 5 shows the calculated phonon frequency distribution. As seen from the figure, due to the heavy mass of the bismuth atom, its phonon frequency distribution has a small energy range. Another interesting observation is the fact that despite that bismuth is a monoatomic crystal, it has an energy gap of width  $\sim 1 \text{ meV}$ . This is due to the deviation of the bismuth structure from a simple cubic, which is similar to the behavior seen in Antimony that has the same structure [10]. Figure 6 shows the total cross section per atom for bismuth at 300 K. Notice that in this calculation the effect of Bragg scattering was neglected. In practice, bismuth is obtained as a filter composed of large poly-crystals. This helps in minimizing the Bragg effect. The figure also shows that the models presented above result in good agreement with experimental data below the Bragg energy cut-off [11-13]. However, above the Bragg cut-off the agreement deteriorates, which may be attributable to the quality of the experimental data.

**Figure 4.** Bismuth (a) Rhombohedral and (b) Hexagonal unit cells.

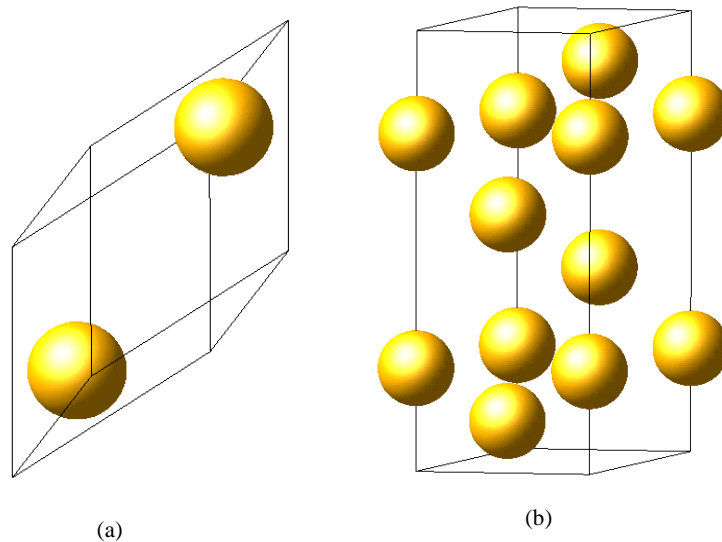


**Figure 5.** The phonon frequency distribution for Bismuth.

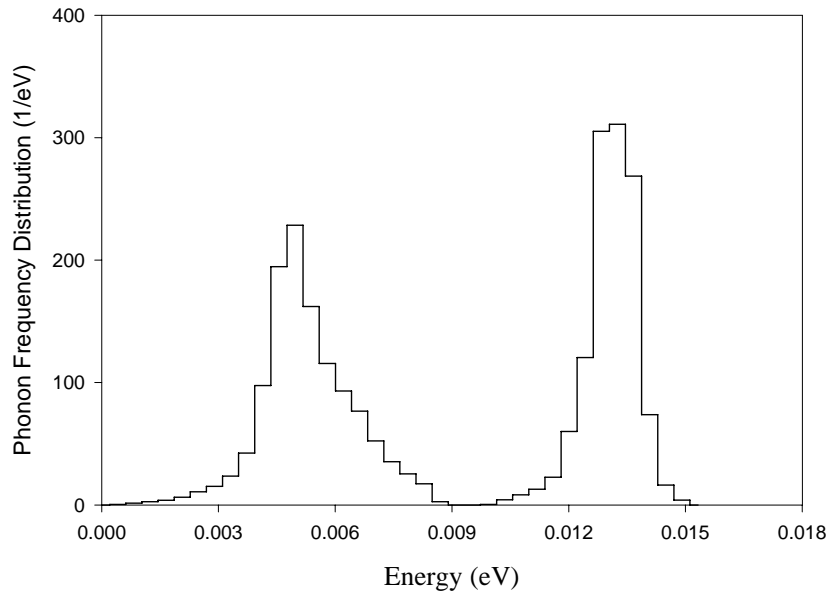
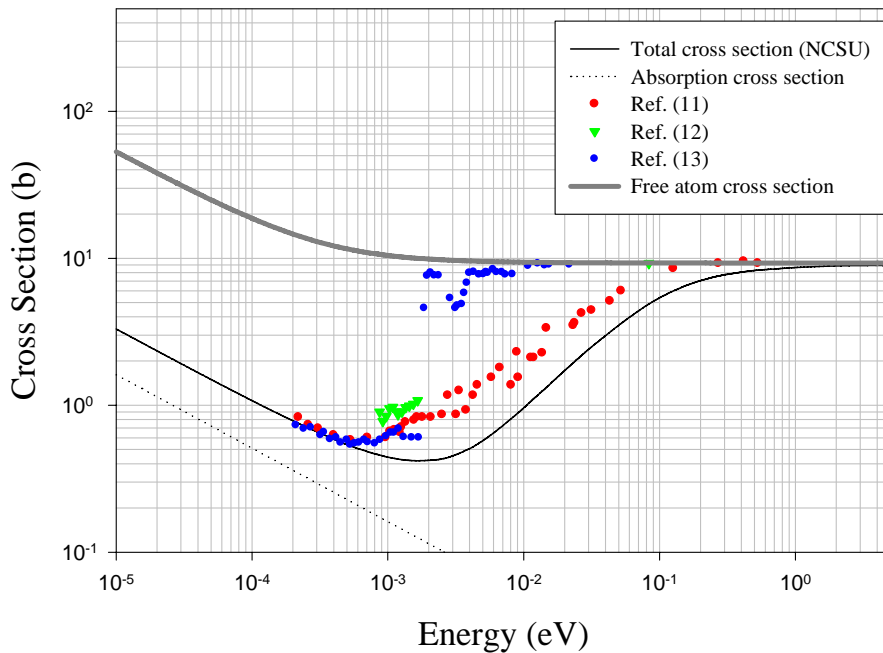


**Figure 6.** The total cross section per atom for a bismuth single crystal at 300 K. Coherent Elastic (Bragg) scattering is not included.



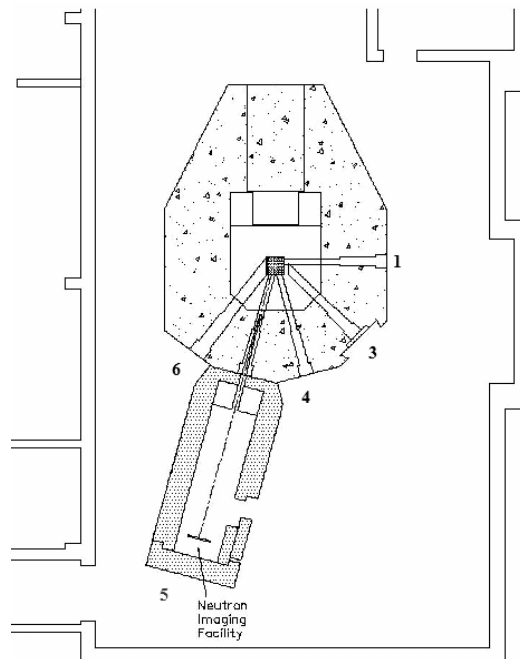
### 3. Neutron Spectrum Simulations

Currently, several experimental facilities that use thermal neutron beams are being set up at the PULSTAR reactor of North Carolina State University (NCSU). The reactor is a swimming pool

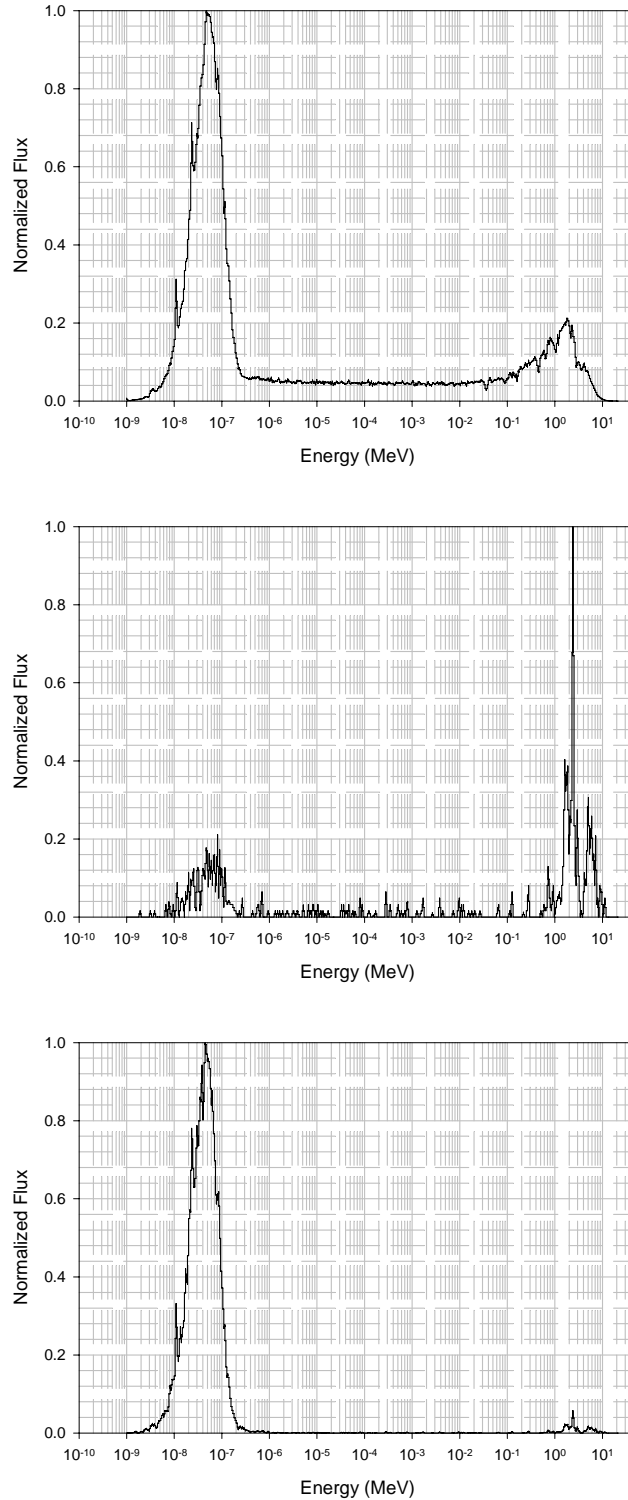
type 1-MWth research reactor with the core placed inside a 15,000 gallon open tank of water. Light water acts as both the coolant and moderator. The core is rectangular and has dimensions of 24x15x13 inches. It is loaded with a 5x5 array of rectangular fuel assemblies. Each fuel assembly includes 25  $\text{UO}_2$  fuel pins enriched to 4% in U-235. To enhance the neutron economy, two sides of the core are reflected by graphite and beryllium. Six beamports are positioned in the pool and provide neutrons for experimental purposes. The layout of the PULSTAR reactor and the arrangement of its beamports are shown in Fig. 7. Several of the experimental facilities that are being set up on the PULSTAR beamports use sapphire and bismuth for neutron and gamma-ray filtration. The MCNP5 code is used to optimize the design of these experiments [14]. For appropriate prediction of the beam characteristics the cross section libraries described above are used in the simulations.

Figure 8 below shows an example of the effect of appropriate modeling of filter effects on the prediction of the neutron spectrum leaking out of beamport #5 (neutron imaging experiment) of the PULSTAR reactor. First, the neutron spectrum leaking from the core is simulated to pass through an open beamport. Second, the core spectrum is simulated to pass through a beam port that contains 4-inches of bismuth followed by 6-inches of sapphire. As the figure illustrates, the use of the standard (free atom) cross section libraries that are supplied with the MCNP5 code (shown in Figures 3 and 6) to describe the interaction of thermal neutrons with sapphire and bismuth results in a drastic underestimation of the flux outside the beamport and a distorted neutron spectrum. However, appropriate accounting of the physics of the interaction of the thermal neutrons in the filter material shows preferential transmission of the neutrons in the thermal energy range, while epithermal and fast neutrons are nearly eliminated. This demonstrates the functionality of the material as a thermal neutron filter.

**Figure 7.** A schematic of the PULSTAR reactor showing the biological shield and the beamports along with the neutron imaging facility on beamport #5. Beamport #2, which is the through port, is not shown.



**Figure 8.** The leakage neutron spectrum form beamport #5 of the PULSTAR reactor without filtration (top), with filtration using free atom cross sections (center), and with filtration using the NCSU cross sections shown in Figures 3 and 6 (bottom).



#### 4. Conclusions

Calculations were performed to investigate the impact of accurate modeling of neutron filter effects on thermal neutron beam simulations. The leakage neutron flux and energy spectrum from beamport #5 of the NCSU PULSTAR research reactor was calculated using the MCNP5 Monte Carlo code. The existence of a 4-inch bismuth filter and a 6-inch sapphire filter was simulated using the standard free atom cross sections. Alternatively, bismuth and sapphire inelastic thermal neutron scattering cross sections were calculated (using the VASP and PHONON codes) and used in the simulations. The generated cross section libraries do not account for coherent elastic (i.e., “Bragg”) scattering, which is equivalent to assuming the use of a single crystal filter with a preferential orientation relative to the neutron beam. It was observed that the use of free atom cross sections resulted in a drastic underestimation of the flux outside the beamport and a distorted neutron energy spectrum. However, appropriate accounting for the physics of the interaction of the thermal neutrons in the filter material shows preferential transmission of the neutrons in the thermal energy range, while epithermal and fast neutrons are nearly eliminated. This illustrates that, using the created libraries, the phenomenon of neutron filtration can be captured and diagnosed to ensure accurate beam and facility designs.

#### Acknowledgements

This work is supported by the US DOE award number DE-FG07-03ID14532.

#### References

- 1) A. I. Hawari, I. I. Al-Qasir, V. H. Gillette, B. W. Wehring, and T. Zhou, “Ab Initio Generation of Thermal Neutron Scattering Cross Sections,” Proceedings of PHYSOR 2004-The Physics of Fuel Cycles and Advanced Nuclear Systems: Global Developments, Chicago, Illinois, 2004.
- 2) D. F. R. Mildner, M. Arif, and C. A. Stone, “Neutron Transmission of Single Crystal Sapphire Filters,” J. Appl. Crystallography, vol. 26, pp. 438-447, 1993.
- 3) D. C. Tennant, “Performance of a Cooled Sapphire and Beryllium Assembly for Filtering of Thermal Neutrons,” Rev. Sci. Instr., vol. 59, pp. 380-381, 1988.
- 4) P. Villars, Pearson's Handbook: Crystallographic Data for Intermetallic Phases, ASM International, Materials Park, OH, 1997.
- 5) R. E. MacFarlane, and D. W. Muir, “The NJOY Nuclear Data Processing System, Version 91,” LA-12740-MS, Los Alamos National Laboratory, 1994.
- 6) R. E. MacFarlane, and D. W. Muir, “New Thermal Neutron Scattering Files for ENDF/B-VI, Release 2,” LA-12639-MS, Los Alamos National Laboratory, 1994.
- 7) G. Kresse, and J. Furthmuller, “Vienna Ab-Initio Simulation Package; VASP the Guide,” Vienna, 2002.
- 8) K. Parlinski, “PHONON Manual, Version 3.11,” Cracow, 2002.
- 9) H. J. Monkhorst, and J. D. Pack, “Special Points for Brillouin Zone Integration,” Phys. Rev. B, vol.13, no. 12, pp. 5188-5192, 1976.
- 10) R. I. Sharp, and E. Warming, “The Lattice Dynamics of Antimony,” J. Phys. F: Metal Physics, vol. 1, pp. 570-587, 1971.

- 11) B. M. Rustad, J. Als-Nielsen, A. Bahnsen, C. J. Christensen, and A. Nielsen, "Single-Crystal Filters for Attenuating Epithermal Neutrons and Gamma Rays in Reactor Beams," *Rev. Sci. Instr.*, vol. 36, pp. 48-54, 1965.
- 12) P. A. Egelstaff, and R. S. Pease, "The design of cold neutron filters," *J. Sci. Instr.*, vol. 31, pp. 207-212, 1954.
- 13) D. J. Hughes, and J. A. Harvey, "Neutron Cross Sections," Brookhaven National Laboratory Report 325, Office of Technical Services, Department of Commerce, Washington D. C., 1955.
- 14) X-5 Monte Carlo Team, "MCNP – A General Monte Carlo N-Particle Transport Code, Version 5," Los Alamos National Laboratory, Los Alamos, NM, Tech. Rep. LA-UR-03-1987, 2003.